Available online at www.eccomasproceedia.org
Eccomas Proceedia COMPDYN (2017) 4691-4701

ECCOMAS
Proceedia

COMPDYN 2017
6th ECCOMAS Thematic Conference on
Computational Methods in Structural Dynamics and Earthquake Engineering
M. Papadrakakis, M. Fragiadakis (eds.)
Rhodes Island, Greece, 15–17 June 2017

# KINEMATIC STRESS RESULTANTS IN INCLINED SINGLE PILES SUBJECTED TO PRAPAGATING SEISMIC WAVES: AN ANALYTICAL FORMULATION

**S. Carbonari[1], M. Morici[2], F. Dezi[3] and G. Leoni[2]**

[1] Università Politecnica delle Marche - DICEA
via Brecce Bianche, Ancona, 60131, Italy
e-mail: s.carbonari@univpm.it

[2] University of Camerino - SAAD
viale della Rimembranza, Ascoli Piceno, 63100, Italy
e-mail: {michele.morici,graziano.leoni}@unicam.it

[3] University of San Marino - DESD
via Salita alla Rocca, San Marino, 47890, San Marino
e-mail: francsca.dezi@unirsm.sm

**Keywords:** Instructions, ECCOMAS Thematic Conference, Structural Dynamics, Earthquake Engineering, Proceedings.

**Abstract.** *This paper presents an analytical model, based on the beam-on-dynamic Winkler foundation approach, for the evaluation of the kinematic stress resultants in single inclined piles subjected to the propagation of seismic waves. The Euler-Bernoulli beam model is adopted for the pile whereas analytical solutions available in literature for viscoelastic layers undergoing harmonic vibrations of a rigid disk are used for the soil. The coupled flexural and axial behaviour of the pile is governed by a system of partial differential equations, with the relevant boundary conditions, that is solved analytically in terms of exponential matrices. The solution for piles embedded in a homogeneous soil deposit is presented. Some applications, including comparisons of results with those obtained from rigorous boundary element formulations, demonstrate that the model, characterised by a very low computational effort, is able to accurately predict stress resultants in inclined piles subjected to seismic loading.*


Peer-review under responsibility of the organizing committee of COMPDYN 2017.
doi: 10.7712/120117.5754.17934

# 1 INTRODUCTION

The Beam-on-Dynamic Winkler Foundation approach (BDWF) has been largely used in the literature to study the problem of a single pile subjected to seismic loading. According to this approach, the soil-pile interaction is captured through the definition of Winkler's coefficients (spring and dashpot coefficients) that may be characterised by a linear or nonlinear behaviour. Despite the nonlinear approach is more suited to model soil-pile interaction phenomena under severe earthquakes, linear approaches are very often preferred for different reasons, the most important of which is the possibility to solve the problem in the frequency domain, where the frequency dependent nature of the soil-pile interaction phenomena can be directly included and convergence problems can be avoided. In this framework, the definition of Winkler's coefficients, able to capture the dynamic stiffness of the soil-pile system and the frequency dependent radiation damping phenomena, constitutes an important task, since they strongly affect both the kinematic and the inertial response of the soil-foundation system [1].

The linear BDWF approach has been used extensively to study the response of vertical piles subjected to dynamic loading for which closed-form solutions, as well as simplified expressions for the prediction of the dynamic stiffness, the kinematic pile response and the maximum bending moments along the pile, have been derived. On the contrary, applications of such approaches to inclined piles are not so popular in the literature and more sophisticated finite element or boundary element models are preferred [2-7].

In this paper an analytical model for the analysis of kinematic stress resultants arising in inclined single piles subjected to the propagation of seismic waves is presented. The model is based on the BDWF approach and an analytical solution of the problem is derived by assuming a linear behaviour of both the pile and soil. In particular, the pile is modelled as a Euler-Bernoulli beam having a generic inclination and the soil-pile interaction is captured by defining soil impedances according to expressions available in the literature for viscoelastic layers undergoing harmonic vibrations of a rigid disk. The coupled flexural and axial behaviour of the pile is described by a system of partial differential equations, with the relevant boundary conditions, that is solved analytically exploiting exponential matrices. Some applications are performed to demonstrate the model efficiency, comparing results, in terms of stress resultants along piles, with those available in the literature, resulting from rigorous boundary element formulations.

# 2 ANALYTICAL MODEL

The analytical formulation of the dynamic problem of a single pile embedded in a homogenous soil deposit and subjected to the free-field seismic displacements is presented in this section. The problem is formulated in the frequency domain by assuming a linear viscoelastic behaviour for the pile and soil.

## 2.1 Kinematics

A single circular pile of diameter $\phi$ and length $L$, embedded with a generic inclination in a homogeneous soil deposit and subjected to a free field motion, is considered and a global orthonormal reference system frame $\{0, x, y, z\}$ is defined with the origin at the top plane of the stratum and the $z$ axis directed downward (Figure 1a). A local reference system $\{0, \xi, \eta, \zeta\}$ of the pile, having the $\zeta$ axis passing through centroids of the circular cross sections, is also introduced.

With reference to points lying on the pile axis, if $\omega$ is the circular frequency, the soil displacements at depth $z$ are described by the complex valued vector

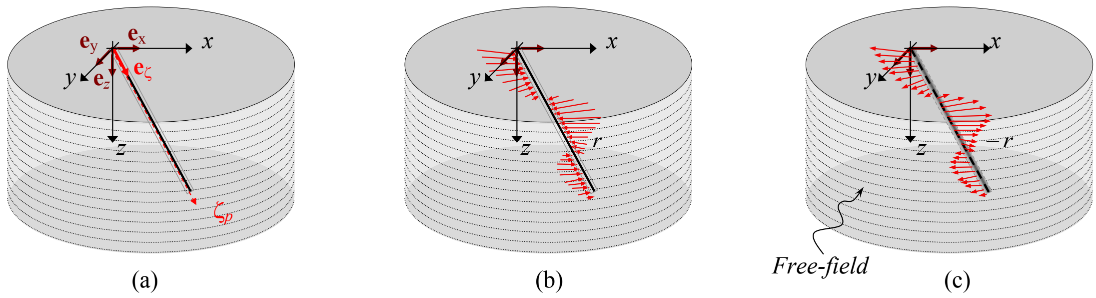


Figure 1: (a): Pile section in the homogeneous stratum; (b) pile section subjected to interaction forces and (c) soil stratum subjected to propagating seismic waves and interaction forces.

$$\mathbf{u}_g(\omega;z)=\begin{bmatrix}\mathbf{u}_h(\omega;z)\\ u_z(\omega;z)\end{bmatrix}_{3\times1} \tag{1}$$

in which sub-vector $\mathbf{u}_h$ groups horizontal components in $x$ and $y$ directions. Similarly, the free-field motion at the pile location $\mathbf{u}_{ff}$ is partitioned by grouping horizontal components in sub-vector $\mathbf{u}_{ff,h}$

$$\mathbf{u}_{ff}(\omega;z)=\begin{bmatrix}\mathbf{u}_{ff,h}(\omega;z)\\ u_{ff,z}(\omega;z)\end{bmatrix}_{3\times1} \tag{2}$$

Under the assumption that no gap between the pile and the soil arises during the motion, pile displacements are conveniently expressed as

$$\mathbf{u}_l(\omega;\zeta)=\mathbf{R}\mathbf{u}_g(\omega;z) \tag{3}$$

where $\mathbf{R}$ is a rotation matrix that allow expressing pile displacements with respect to the local reference system, starting from displacements expressed with respect to the global one. According to the Euler-Bernoulli model, the displacement field of the generic point of the pile cross-section can be obtained from

$$\mathbf{s}_l^T(\omega;\xi,\eta,\zeta)=\begin{bmatrix}\mathbf{u}_t(\omega;\zeta)\\ u_\zeta(\omega;\zeta)-\mathbf{u}_t'(\omega;\zeta)\cdot\mathbf{a}(\xi,\eta)\end{bmatrix}_{3\times1} \tag{4}$$

where prime denotes derivatives with respect to $\zeta$ and $\mathbf{a}(\xi,\eta)=[\xi,\eta]^T$ is the vector of local coordinates $\xi$ and $\eta$ of the cross section generic point. The pile undergoes only the longitudinal normal strain

$$\varepsilon_\zeta(\omega;\xi,\eta,\zeta)=u_\zeta'(\omega;\zeta)-\mathbf{u}_t''(\omega;\zeta)\cdot\mathbf{a}(\xi,\eta) \tag{5}$$

## 2.2 Viscoelastic linear problem

The pile is constituted by a linear viscoelastic material, characterized by Young's modulus $E_p$ and material damping $\delta_p$, taken into account according to the correspondence principle [8]. During the motion, the pile interacts with the surrounding soil and resultants of the soil reactions are assumed to be constituted by forces distributed along the pile.

By grouping the horizontal components of the soil reaction resultants in sub-vector $\mathbf{r}_h$, and denoting by $r_z$ the vertical component, vector of the line reaction forces is (Figure 1b)

$$\mathbf{r}(\omega; z) = \begin{bmatrix} \mathbf{r}_h(\omega; z) \\ r_z(\omega; z) \end{bmatrix}_{3\times 1} \tag{6}$$

By considering the soil stratum constituted by infinite horizontal independent layers with linear viscoelastic behaviour, reaction forces are given by (Figure 1c)

$$\mathbf{r}(\omega; z) = \Im(\omega)\left[\mathbf{u}_{ff}(\omega; z) - \mathbf{u}_g(\omega; z)\right] \tag{7}$$

where $\Im$ is the 3x3 impedance matrix of the unbounded soil layers. Matrix $\Im$ can be populated considering results of studies by Dobry et al. [9], Makris and Gazetas [10] and Gazetas and Dobry [11]. Components of matrix $\Im$ represent forces necessary to induce unitary harmonic vibrations of a rigid disk at depth $z$. The equilibrium condition of the pile may be expressed by the Lagrange-D'Alembert principle that, suitably integrated by parts, furnishes

$$\begin{aligned} & E_p^*\left(\mathbf{J}\int_0^L \mathbf{u}_t'''' \cdot \hat{\mathbf{u}}_t d\zeta - A\int_0^L u_\zeta'' \hat{u}_\zeta d\zeta\right) - \omega^2\rho_p\left(A\int_0^L \mathbf{u}_t \cdot \hat{\mathbf{u}}_t \mathrm{d}\zeta + A\int_0^L u_\zeta \hat{u}_\zeta \mathrm{d}\zeta - \mathbf{J}\int_0^L \mathbf{u}_t'' \cdot \hat{\mathbf{u}}_t \mathrm{d}\zeta\right) \\ & + \int_0^L \left(\mathbf{R}\Im\mathbf{R}^T\mathbf{u}_l \cdot \hat{\mathbf{u}}_l\right) c_{z\zeta}\mathrm{d}\zeta - \int_0^L \left(\mathbf{R}\Im\mathbf{u}_{ff} \cdot \hat{\mathbf{u}}_l\right) c_{z\zeta}\mathrm{d}\zeta + E_p^*\left(Au_\zeta'\hat{u}_\zeta + \mathbf{J}\mathbf{u}_t'' \cdot \hat{\mathbf{u}}_t' - \mathbf{J}\mathbf{u}_t''' \cdot \hat{\mathbf{u}}_t\right)\Big|_0^L \\ & - \omega^2\rho_p\left(\mathbf{J}\mathbf{u}_t' \cdot \hat{\mathbf{u}}_t\right)\Big|_0^L - \left(\mathbf{F}_t \cdot \hat{\mathbf{u}}_t + F_\zeta\hat{u}_\zeta + \mathbf{M}_t \cdot \hat{\mathbf{u}}_t'\right)\Big|_0 - \left(\mathbf{F}_t \cdot \hat{\mathbf{u}}_t + F_\zeta\hat{u}_\zeta + \mathbf{M}_t \cdot \hat{\mathbf{u}}_t'\right)\Big|_L = 0 \qquad \forall\hat{\mathbf{u}}_l \neq \mathbf{0} \end{aligned} \tag{8}$$

where $\mathbf{J}$ is the inertia matrix and $A$ is the area of the pile cross section, respectively, while $E_p^*=E_p(1+2i\delta_p)$ is the complex elastic modulus of the pile material [8]. From Equation (8), according to the fundamental theorem of variational calculus, the local balance conditions

$$\begin{aligned} & E_p^*\mathbf{J}\mathbf{u}_t'''' + \omega^2\rho_p\mathbf{J}\mathbf{u}_t'' - \omega^2\rho_p A\mathbf{u}_t + c_{z\zeta}\underset{1,2}{\overset{1,2}{\mathsf{S}}}\left(\mathbf{R}\Im\mathbf{R}^T\right)\mathbf{u}_t + c_{z\zeta}\underset{1,2}{\overset{3}{\mathsf{S}}}\left(\mathbf{R}\Im\mathbf{R}^T\right)u_\zeta \\ & \qquad = c_{z\zeta}\underset{1,2}{\overset{1,2}{\mathsf{S}}}\left(\mathbf{R}\Im\right)\mathbf{u}_{ff,h} + c_{z\zeta}\underset{1,2}{\overset{3}{\mathsf{S}}}\left(\mathbf{R}\Im\right)u_{ff,z} \\ & -E_p^*Au_\zeta'' - \omega^2\rho_p Au_\zeta + c_{z\zeta}\underset{3}{\overset{1,2}{\mathsf{S}}}\left(\mathbf{R}\Im\mathbf{R}^T\right)\mathbf{u}_t + c_{z\zeta}\underset{3}{\overset{3}{\mathsf{S}}}\left(\mathbf{R}\Im\mathbf{R}^T\right)u_\zeta \\ & \qquad = c_{z\zeta}\underset{3}{\overset{1,2}{\mathsf{S}}}\left(\mathbf{R}\Im\right)\mathbf{u}_{ff,h} + c_{z\zeta}\underset{3}{\overset{3}{\mathsf{S}}}\left(\mathbf{R}\Im\right)u_{ff,z} \end{aligned} \tag{9}$$

as well as the relevant boundary conditions

$$\begin{aligned} & \left(E_p^*Au_\zeta' + F_\zeta\right)\hat{u}_\zeta\Big|_0 = 0 \quad \forall\hat{u}_\zeta & & \left(E_p^*Au_\zeta' - F_\zeta\right)\hat{u}_\zeta\Big|_L = 0 \quad \forall\hat{u}_\zeta \\ & \left(E_p^*\mathbf{J}\mathbf{u}_t''' + \omega^2\rho_p\mathbf{J}\mathbf{u}_t' - \mathbf{F}_t\right)\cdot\hat{\mathbf{u}}_t\Big|_0 = 0 \quad \forall\hat{\mathbf{u}}_t & & \left(E_p^*\mathbf{J}\mathbf{u}_t''' + \omega^2\rho_p\mathbf{J}\mathbf{u}_t' + \mathbf{F}_t\right)\cdot\hat{\mathbf{u}}_t\Big|_L = 0 \quad \forall\hat{\mathbf{u}}_t \\ & \left(E_p^*\mathbf{J}\mathbf{u}_t'' + \mathbf{M}_t\right)\cdot\hat{\mathbf{u}}_t'\Big|_0 = 0 \quad \forall\hat{\mathbf{u}}_t' & & \left(E_p^*\mathbf{J}\mathbf{u}_t'' - \mathbf{M}_t\right)\cdot\hat{\mathbf{u}}_t'\Big|_L = 0 \quad \forall\hat{\mathbf{u}}_t' \end{aligned} \tag{10}$$

are derived. In equations (9), $\underset{i,j}{\overset{l,m}{\mathsf{S}}}\mathbf{A}$ indicates segments of a generic matrix $\mathbf{A}$ constituted by the subset of rows comprised between $i$ and $j$ and the subset of columns comprised between $l$ and $m$. Equations (9) is a system of ordinary differential equations with constant coefficients whose unknowns are the complex valued function $\mathbf{u}_l(\zeta)$ fulfilling the boundary conditions (10) that encompass both kinematic and static conditions.

$$\mathbf{x}(\omega;\zeta)=\begin{bmatrix}\mathbf{u}_t\\ u_\zeta\\ \mathbf{u}'_t\\ u'_\zeta\\ \mathbf{u}''_t\\ \mathbf{u}'''_t\end{bmatrix}_{10\times 1} \tag{11}$$

System (9), with the boundary conditions (10), can be thus rewritten in the canonical form

$$\mathbf{x}'-\mathbf{B}(\omega)\mathbf{x}=\mathbf{c}(\omega;\zeta) \tag{12}$$

$$\begin{aligned}&\left[\mathbf{D}(\omega)\mathbf{x}+\mathbf{P}(\omega)\right]\cdot \mathop{\mathrm{S}}_{1,5}^{1}\hat{\mathbf{x}}\Big|_0=\mathbf{0} \qquad \forall\hat{\mathbf{x}}\\ &\left[\mathbf{D}(\omega)\mathbf{x}-\mathbf{P}(\omega)\right]\cdot \mathop{\mathrm{S}}_{1,5}^{1}\hat{\mathbf{x}}\Big|_L=\mathbf{0} \qquad \forall\hat{\mathbf{x}}\end{aligned} \tag{13}$$

where

$$\mathbf{B}=\begin{bmatrix}\mathbf{0} & \mathbf{0} & \mathbf{I}_2 & \mathbf{0} & \mathbf{0} & \mathbf{0}\\ \mathbf{0} & 0 & \mathbf{0} & 1 & \mathbf{0} & \mathbf{0}\\ \mathbf{0} & \mathbf{0} & \mathbf{0} & \mathbf{0} & \mathbf{I}_2 & \mathbf{0}\\ \dfrac{c_{z\zeta}}{E_p^*A}\mathop{\mathrm{S}}_{3}^{1,2}\left(\mathbf{R}\Im\mathbf{R}^T\right) & \dfrac{c_{z\zeta}}{E_p^*A}\mathop{\mathrm{S}}_{3}^{3}\left(\mathbf{R}\Im\mathbf{R}^T\right)-\dfrac{\omega^2\rho_p}{E_p^*} & \mathbf{0} & 0 & \mathbf{0} & \mathbf{0}\\ \mathbf{0} & \mathbf{0} & \mathbf{0} & \mathbf{0} & \mathbf{0} & \mathbf{I}_2\\ \dfrac{\omega^2\rho_p}{E_p^*}A\mathbf{J}^{-1}-\dfrac{c_{z\zeta}}{E_p^*}\mathbf{J}^{-1}\mathop{\mathrm{S}}_{1,2}^{1,2}\left(\mathbf{R}\Im\mathbf{R}^T\right) & -\dfrac{c_{z\zeta}}{E_p^*}\mathbf{J}^{-1}\mathop{\mathrm{S}}_{1,2}^{3}\left(\mathbf{R}\Im\mathbf{R}^T\right) & \mathbf{0} & \mathbf{0} & -\dfrac{\omega^2\rho_p}{E_p^*}\mathbf{I}_2 & \mathbf{0}\end{bmatrix} \tag{14}$$

$$\mathbf{D}=\begin{bmatrix}\mathbf{0} & 0 & -\omega^2\rho_p\mathbf{J} & 0 & \mathbf{0} & -E_p^*\mathbf{J}\\ \mathbf{0} & 0 & \mathbf{0} & E_p^*A & \mathbf{0} & \mathbf{0}\\ \mathbf{0} & 0 & \mathbf{0} & 0 & E_p^*\mathbf{J} & \mathbf{0}\end{bmatrix} \tag{15}$$

are complex valued matrices, depending on the stiffness of the pile cross section and on the impedance of the soil layers, while

$$\mathbf{c}=\begin{bmatrix}\mathbf{0}\\ 0\\ \mathbf{0}\\ -\dfrac{1}{E_p^*A}\left(c_{z\zeta}\mathop{\mathrm{S}}_{3}^{1,2}\left(\mathbf{R}\Im\right)\mathbf{u}_{ff,h}+c_{z\zeta}\mathop{\mathrm{S}}_{3}^{3}\left(\mathbf{R}\Im\right)u_{ff,z}\right)\\ \mathbf{0}\\ \dfrac{1}{E_p^*}\mathbf{J}^{-1}\left(c_{z\zeta}\mathop{\mathrm{S}}_{1,2}^{1,2}\left(\mathbf{R}\Im\right)\mathbf{u}_{ff,h}+c_{z\zeta}\mathop{\mathrm{S}}_{1,2}^{3}\left(\mathbf{R}\Im\right)u_{ff,z}\right)\end{bmatrix} \tag{16}$$

$$\mathbf{P}=\begin{bmatrix}\mathbf{F}_t\\ F_\zeta\\ \mathbf{M}_t\end{bmatrix} \tag{17}$$

are vectors depending on distributed soil-pile reaction forces and loads concentrated at the pile ends, respectively.

Equation (12) is a linear system of ordinary differential equations with constant coefficients whose general solution is obtained by summing the complementary solution (solution of the associate homogeneous equation) to a particular solution depending on the external loads. It can be demonstrated that such a solution may be written as

$$\mathbf{x} = \mathbf{E}(\omega;\zeta)\mathbf{g}(\omega) + \mathbf{E}(\omega;\zeta)\int \mathbf{E}^{-1}(\omega;\zeta)\mathbf{c}\,d\zeta \tag{18}$$

where $\mathbf{E}$ is the exponential matrix defined through a series expansion by

$$\mathbf{E}(\omega;\zeta) = \sum_{k=0}^{\infty} \frac{1}{k!}\mathbf{B}^k(\omega)\zeta^k \tag{19}$$

and $\mathbf{g}$ is the vector of the integration constants that has to be calculated from the boundary conditions (13). Equation (18) is of general validity and the evaluation of the particular solution requires to know the expression of the free field motion; in this paper the case of one-dimensional propagation of shear and pressure waves in the vertical direction is considered. These are governed by expressions

$$\mathbf{u}_{ff,h}(\omega; z) = \mathbf{q}_h(\omega)e^{ik_h z} + \mathbf{t}_h(\omega)e^{-ik_h z} \tag{20}$$

$$u_{ff,z}(\omega; z) = q_z(\omega)e^{ik_z z} + t_z(\omega)e^{-ik_z z} \tag{21}$$

where

$$k_h = \sqrt{\frac{\omega^2}{V_s^2(1+2i\delta_s)}} \qquad k_z = \sqrt{\frac{\omega^2}{V_{La}^2(1+2i\delta_s)}} \tag{22}$$

are the complex wavenumbers associated to the propagation of shear and pressure waves, respectively, and $\mathbf{q}_h$, $\mathbf{t}_h$, $q_z$ and $t_z$ are integration constants depending on the boundary conditions (i.e. at the ground surface and at the bedrock level) [12]. Taking into account equation (16)

$$\mathbf{c} = \mathbf{Q}_h(\omega)e^{ik_h c_{z\zeta}\zeta} + \mathbf{T}_h(\omega)e^{-ik_h c_{z\zeta}\zeta} + \mathbf{Q}_z(\omega)e^{ik_z c_{z\zeta}\zeta} + \mathbf{T}_z(\omega)e^{-ik_z c_{z\zeta}\zeta} \tag{23}$$

where

$$\mathbf{Q}_h(\omega) = \begin{bmatrix} \mathbf{0} \\ 0 \\ \mathbf{0} \\ -\dfrac{c_{z\zeta}}{E_p^* A} \overset{1,2}{\underset{3}{\mathsf{S}}}(\mathbf{R}\Im)\mathbf{q}_h \\ \mathbf{0} \\ \dfrac{c_{z\zeta}}{E_p^*}\mathbf{J}^{-1} \overset{1,2}{\underset{1,2}{\mathsf{S}}}(\mathbf{R}\Im)\mathbf{q}_h \end{bmatrix} \qquad \mathbf{T}_h(\omega) = \begin{bmatrix} \mathbf{0} \\ 0 \\ \mathbf{0} \\ -\dfrac{c_{z\zeta}}{E_p^* A} \overset{1,2}{\underset{3}{\mathsf{S}}}(\mathbf{R}\Im)\mathbf{t}_h \\ \mathbf{0} \\ \dfrac{c_{z\zeta}}{E_p^*}\mathbf{J}^{-1} \overset{1,2}{\underset{1,2}{\mathsf{S}}}(\mathbf{R}\Im)\mathbf{t}_h \end{bmatrix} \tag{24}$$

$$\mathbf{Q}_z(\omega)=\begin{bmatrix} \mathbf{0} \\ 0 \\ \mathbf{0} \\ -\frac{c_{z\zeta}}{E_p^* A} \mathop{\mathsf{S}}_{3}^{3} (\mathbf{R}\Im) q_z \\ \mathbf{0} \\ \frac{c_{z\zeta}}{E_p^*} \mathbf{J}^{-1} \mathop{\mathsf{S}}_{1,2}^{3} (\mathbf{R}\Im) q_z \end{bmatrix} \qquad \mathbf{T}_z(\omega)=\begin{bmatrix} \mathbf{0} \\ 0 \\ \mathbf{0} \\ -\frac{c_{z\zeta}}{E_p^* A} \mathop{\mathsf{S}}_{3}^{3} (\mathbf{R}\Im) t_z \\ \mathbf{0} \\ \frac{c_{z\zeta}}{E_p^*} \mathbf{J}^{-1} \mathop{\mathsf{S}}_{1,2}^{3} (\mathbf{R}\Im) t_z \end{bmatrix} \tag{25}$$

By substituting (23) in (18) yields

$$\mathbf{x} = \mathbf{E}\mathbf{g}_f + \mathbf{E}\int \mathbf{E}^{-1}\left(\mathbf{Q}_h e^{ik_h c_{z\zeta}\zeta} + \mathbf{T}_h e^{-ik_h c_{z\zeta}\zeta} + \mathbf{Q}_z e^{ik_z c_{z\zeta}\zeta} + \mathbf{T}_z e^{-ik_z c_{z\zeta}\zeta}\right) d\zeta \tag{26}$$

which, for properties of exponential matrix, can be rewritten as

$$\mathbf{x} = \mathbf{E}\mathbf{g}_f + \widetilde{\mathbf{x}}_h + \widetilde{\mathbf{x}}_z \tag{27}$$

where

$$\widetilde{\mathbf{x}}_h = \mathbf{E}\left[\left(ik_h c_{z\zeta}\mathbf{I} - \mathbf{B}\right)^{-1}\mathbf{E}^{-1}\mathbf{Q}_h e^{ik_h c_{z\zeta}\zeta} - \left(ik_h c_{z\zeta}\mathbf{I} + \mathbf{B}\right)^{-1}\mathbf{E}^{-1}\mathbf{T}_h e^{-ik_h c_{z\zeta}\zeta}\right] \tag{28}$$

$$\widetilde{\mathbf{x}}_z = \mathbf{E}\left[\left(ik_z c_{z\zeta}\mathbf{I} - \mathbf{B}\right)^{-1}\mathbf{E}^{-1}\mathbf{Q}_z e^{ik_z c_{z\zeta}\zeta} - \left(ik_z c_{z\zeta}\mathbf{I} + \mathbf{B}\right)^{-1}\mathbf{E}^{-1}\mathbf{T}_z e^{-ik_z c_{z\zeta}\zeta}\right] \tag{29}$$

are the particular solutions for shear and pressure waves propagating in the vertical direction, respectively. Differently from classical numerical methods (e.g finite element method and finite difference method), this approach allows expressing the problem solution analytically; in the case of homogeneous soil deposit the discretization of the pile axis is not needed to achieve an accurate numerical solution.

Once the solution is determined, stress resultants in the pile can be obtained with

$$\begin{bmatrix} N(\omega;\zeta) \\ M_\eta(\omega;\zeta) \\ M_\xi(\omega;\zeta) \\ V_\xi(\omega;\zeta) \\ V_\eta(\omega;\zeta) \end{bmatrix} = E_p^* \frac{\pi\phi^4}{64} \begin{bmatrix} 0 & 0 & \frac{16}{\phi^2} & 0 & 0 & 0 & 0 \\ 0 & 0 & 0 & 1 & 0 & 0 & 0 \\ 0 & 0 & 0 & 0 & -1 & 0 & 0 \\ -\omega^2\frac{\rho_p}{E_p^*} & 0 & 0 & 0 & 0 & -1 & 0 \\ 0 & -\omega^2\frac{\rho_p}{E_p^*} & 0 & 0 & 0 & 0 & -1 \end{bmatrix} \mathop{\mathsf{S}}_{4,10}^{1} \mathbf{x}(\omega;\zeta) \tag{30}$$

## 3 APPLICATIONS

In this section, some applications are presented in order to show the model potential in capturing the kinematic stress resultants in inclined piles subjected to propagating seismic waves. For this proposes, results of some applications available in Padron et al. [5], performed with a boundary element model, are considered as benchmarks. The adopted geometrical and mechanical parameters are reported in Figure 2; applications are performed considering 12 m long piles with different inclination (θ = 0°, 10°, 20°, 30°) embedded in a homogeneous soil deposit characterised by two different shear wave velocites ($V_s$ = 250 and 110 m/s). The pile Young's modulus and density are $E_p$ = 30000 MPa and $\rho_p$ = 2.5 t/m$^3$, respectively. The seismic input at the ground surface is constituted by an artificial accelerogram with a peak ground acceleration $a_g$ = 0.375g, individually matching the elastic response spectrum for ground type C and 5% damping. This has been obtained according to the Gasparini & Vanmarcke spectrum-compatible nonstationary ground motion model [13]. The seismic action is applied in the $x$ direction. For this applications the pile is not subdivided and the Lysmer's analogue velocity is assumed for the compression waves within the whole pile.

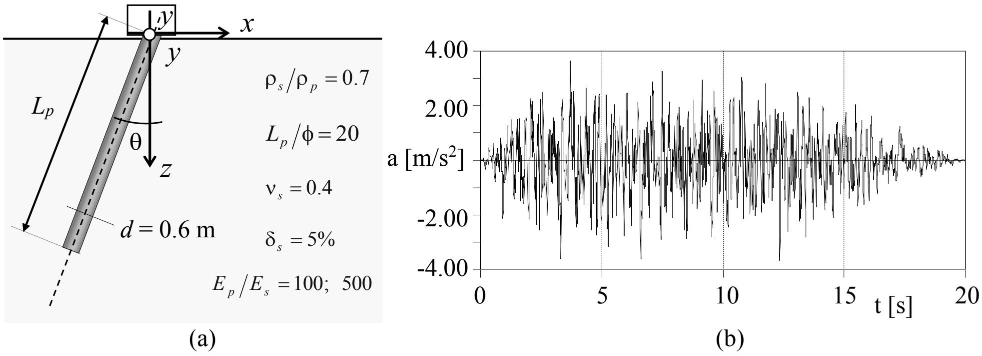


Figure 1: (a) Pile geometry and (b) seismic input.

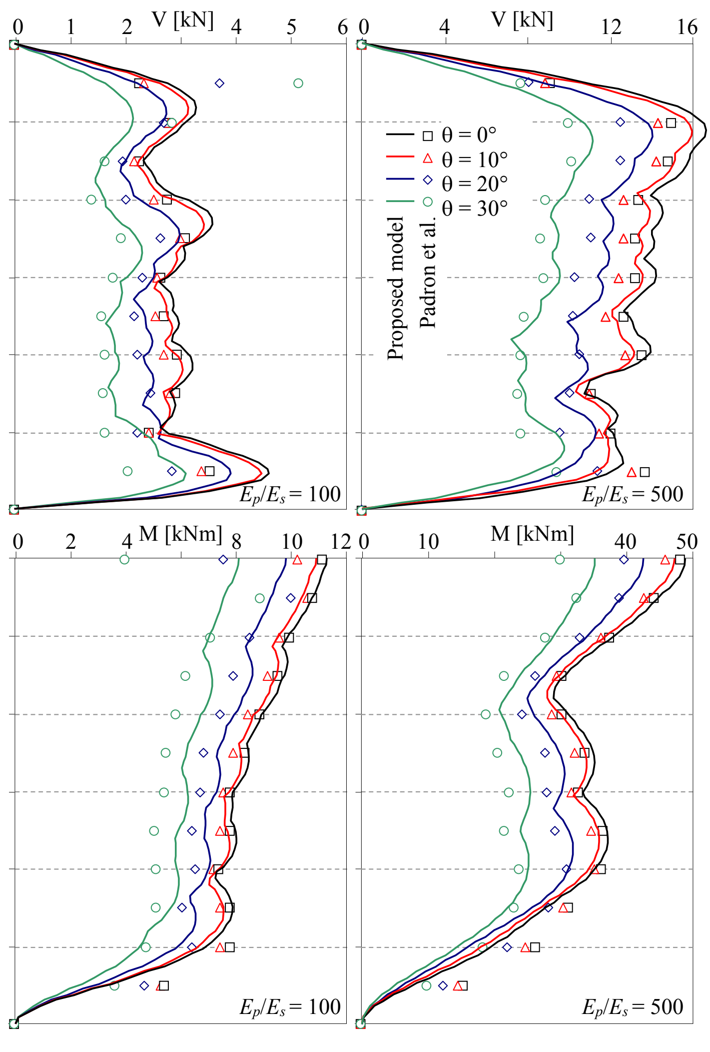


Figure 2: (a) Envelops of absolute kinematic shear force and bending moments along the pile.

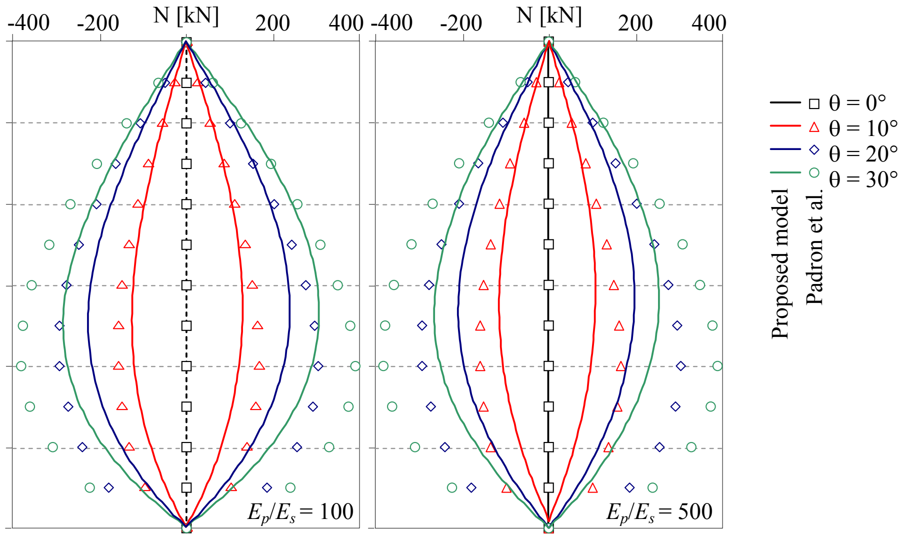


Figure 3: Envelops of maximum and minimum axial force along the pile.

Figure 3 shows the envelopes of absolute values of shear forces and bending moments arising along the pile as a consequence of the kinematic interaction. Results obtained by considering different pile inclinations are reported with curves of different colours for both the investigated soil deposits, characterised by pile-soil modulus ratios $E_p/E_s = 100$ ($V_s = 250$ m/s) and $E_p/E_s = 500$ ($V_s = 110$ m/s). Furthermore, benchmarks are reported with marks while continuous lines are used for results of the proposed formulation. For both pile-soil modulus ratios benchmark shear forces are overall well reproduced, independently on the pile rake angle. However, with reference to $E_p/E_s = 100$ significant differences are evident in proximity of the pile head and also nearby the pile base; in particular, benchmark shear forces are higher than those evaluated with the proposed approach at the pile head and slightly lower at the pile base. Local inconsistency at the pile head is probably due to the adopted local soil-pile impedances, based on the plane-strain assumption, which are not able to capture the dynamics of soil layers near the ground surface, characterised by a reduced degree of confinement and by the propagation of surface waves. Previous observation is confirmed by results of $E_p/E_s = 500$, namely of a softer soil, for which shear forces arising in proximity of the pile head are better captured. As for bending moments, the benchmarks are well reproduced for both soil conditions ($E_p/E_s = 100$, 500) expect for the local inconsistencies in proximity of the pile head where bending moments resulting from the BE approach tend to reduce, probably as a consequence of the minor degree of confinement exerted by the superficial soil. As explained above, this effect cannot be captured by the proposed model unless different local soil-pile impedances, suitably calibrated to capture these phenomena, are implemented. As expected, discrepancies between benchmarks and the present results at the pile head reduce in the case of softer soils ($E_p/E_s = 500$). Anyway, bending moments at the head appear to be consistent as they are characterised by a vertical tangent, according to the null value of shear force.

Figure 4 shows the envelopes of maximum and minimum axial forces along the pile obtained from the applications. Maximum discrepancies of about 25÷30% between benchmarks and the proposed solution are observed for both soil conditions ($E_p/E_s = 100$, 500), mainly concentrated in the lower half-length of the pile.

From an overall standpoint, kinematic shear forces and bending moments induced by the seismic wave propagation reduce by increasing the pile rake angle, independently on the soil stiffness, while, as expected, axial forces increase.

## 4 CONCLUSIONS

An analytical model, based on the BDWF approach, for the evaluation of kinematic stress resultants arising in inclined single piles subjected to the propagation of seismic waves in the soil has been presented. The pile is modelled as a Euler-Bernoulli beam having a generic inclined configuration and the soil-pile interaction is captured exploiting elastodynamic solutions available in the literature. The coupled flexural and axial problem is solved analytically exploiting exponential matrices and analytical expressions of kinematic stress resultants are provided. The model is characterised by a computational effort much lower than that associated with numerical solutions formulated with the finite element or boundary element methods.

Some applications are performed comparing results with those available in the literature, derived from rigorous boundary element solutions. Results demonstrate that shear forces and bending moments along the pile resulting from more rigorous approaches, are well reproduced, independently on the pile rake angle and soil conditions (overall errors of about 10% are obtained). However, local inconsistencies at the pile head are observed; these may be due to the adopted elastodynamic solutions to model the soil-pile interaction. As for axial forces, greater discrepancies with benchmarks (ranging between 25÷30%) are evident for both soil conditions, mainly concentrated in the lower half-length of the pile.

## REFERENCES


[1] G. Mylonakis, A. Nikolaou, G. Gazetas, Soil–pile–bridge interaction: kinematic and inertial effects. Part I: soft soil. *Earthquake Engng Struct. Dynamics*, **26**(3), 337–359, 1997.

[2] N. Gerolymos, A. Giannakou, I. Anastasopoulos, G. Gazetas, Evidence of beneficial role of inclined piles: observations and summary of numerical analyses. *Bulletin of Earthquake Engineering*, **6**(4), 705–722, 2008.

[3] A. Giannakou, N. Gerolymos, G. Gazetas, T. Tazoh, I. Anastasopoulos, Seismic Behavior of Batter Piles: Elastic Response. *Journal of Geotechnical and Geoenvironmental Engineering*, **136**, 1187–1199, 2010.

[4] L.A. Padrón, J.J. Aznárez, O. Maeso, A. Santana, Dynamic stiffness of deep foundations with inclined piles. *Earthquake Engng Struct. Dynamics*, **39**(12), 1343–1367, 2010.

[5] L.A. Padrón, A. Suárez, J.J. Aznárez, O. Maeso, Kinematic internal forces in deep foundations with inclined piles. *Earthquake Engng. Struct. Dynamics*, **44**(12), 2129–2135, 2015.

[6] C. Medina, L.A. Padrón, J.J. Aznárez, A. Santana, O. Maeso, Kinematic interaction factors of deep foundations with inclined piles. *Earthquake Engng. Struct. Dynamics*, **43**(13), 2035–2050, 2014.

[7] F. Dezi, S. Carbonari, M. Morici, A Numerical Model for the Dynamic Analysis of Inclined Pile Groups. *Earthquake Engng Struct. Dynamics*, **45**(1), 45–68, 2016.

[8] N. Makris, Causal hysteretic element. *Journal of Engineering Mechanics, ASCE,* **123**(11): 1209–1214, 1997.

[9] R. Dobry, E. Vicente, M.J. O'Rourke, J.M. Roesset, Horizontal Stiffness and Damping of Single Piles. *Journal of Geotechnical Engineering Division, ASCE*, **108**(GT3), 439–459, 1982.

[10] N. Makris, G. Gazetas, Displacement phase differences in a harmonically oscillating pile. *Geotechnique*, **43**(1), 135–150, 1993.

[11] G. Gazetas, R. Dobry, Single radiation damping model for piles and footings. *J. Engng. Mech., ASCE*, **110**(6), 937–956, 1984.

[12] S.L. Kramer, *Geotechnical Earthquake Engineering*. Prentice Hall, Upper Saddle River, RJ, 1996

[13] D.A. Gasparini, E.H. Vanmarcke, Evaluation of Seismic Safety of Buildings – Simulated Earthquake Motions with Prescribed Response Spectra. Massachusetts Institute of Technology, Report No.2, 1976.